Published online October 27, 2004

Nucleic Acids Research, 2004, Vol. 32, No. 19 ***5757–5765***
doi:10.1093/nar/gkh862

Application of locked nucleic acids to improve aptamer *in vivo* stability and targeting function

Kathrin S. Schmidt, Sandra Borkowski[1], Jens Kurreck, Andrew W. Stephens[1], Rolf Bald, Maren Hecht[1], Matthias Friebe[1], Ludger Dinkelborg[1] and Volker A. Erdmann*

Institute of Chemistry (Biochemistry), Free University Berlin, Thielallee 63, D-14195 Berlin, Germany and [1]Research Laboratories Schering AG, 13342 Berlin, Germany

Received June 25, 2004; Revised August 27, 2004; Accepted September 14, 2004

ABSTRACT

Aptamers are powerful candidates for molecular imaging applications due to a number of attractive features, including rapid blood clearance and tumor penetration. We carried out structure–activity relationship (SAR) studies with the Tenascin-C binding aptamer TTA1, which is a promising candidate for application in tumor imaging with radioisotopes. The aim was to improve its *in vivo* stability and target binding. We investigated the effect of thermal stabilization of the presumed non-binding double-stranded stem region on binding affinity and resistance against nucleolytic degradation. To achieve maximal thermal stem stabilization melting experiments with model hexanucleotide duplexes consisting of unmodified RNA, 2′-*O*-methyl RNA (2′-OMe), 2′-Fluoro RNA (2′-F) or Locked Nucleic Acids (LNAs) were initially carried out. Extremely high melting temperatures have been found for an LNA/LNA duplex. TTA1 derivatives with LNA and 2′-OMe modifications within the non-binding stem have subsequently been synthesized. Especially, the LNA-modified TTA1 derivative exhibited significant stem stabilization and markedly improved plasma stability while maintaining its binding affinity to the target. In addition, higher tumor uptake and longer blood retention was found in tumor-bearing nude mice. Thus, our strategy to introduce LNA modifications after the selection procedure is likely to be generally applicable to improve the *in vivo* stability of aptamers without compromising their binding properties.

INTRODUCTION

Aptamers are able to bind with high affinity and selectivity to many diverse types of target molecules, such as small molecules, peptides, proteins, viral particles and even whole cells (1–4) with dissociation constants down to picomolar values. This is due to their ability to form elaborate three-dimensional structures. Consisting of nucleic acids, aptamers are selected from a large combinatorial library by a process of iterative selection and amplification. This method is referred to as Systematic Evolution of Ligands by Exponential Enrichment (SELEX) (5–7). The molecular weight of aptamers (10–15 kDa) is one order of magnitude lower than that of antibodies (150 kDa) (8), hence aptamers are expected to have rapid tissue and tumor penetration, as well as fast blood clearance. In contrast to antibodies, aptamers are non-immunogenic and can display favorable target-to-noise ratios at early time points. Thus, aptamers exhibit many characteristics desired for non-invasive *in vivo* tumor imaging and therapy (9–11). In addition, aptamers, which are fully synthetic molecules, allow both rapid analoging for structure–activity relationship (SAR) studies and site-specific modification and conjugation for the attachment of unique chelating molecules, photoactive probes, radionuclides, drugs and pharmacokinetic modifying agents (12–15).

Prerequisites for a successful *in vivo* application of aptamers as molecular target imaging agents are represented by high affinity and selectivity to their target as well as by adequate stability against *in vivo* degradation. A number of strategies have been employed to stabilize aptamers against 3′ and 5′ exonucleases as well as endonucleases, while maintaining target affinity. Chemical modifications at the 2′ position of the ribose moiety, circularization of the aptamer, 3′ capping and 'spiegelmer' technology have been described (8,16–20). Another crucial issue is the conformational stability of an aptamer *in vivo*. Conformational flexibility is hypothesized to be a major factor limiting the affinity and specificity of interactions due to the entropic penalty upon binding (21). Furthermore, since single-stranded regions are the primary site of nuclease attack, conformational flexibility would render the aptamer more accessible to nucleolytic degradation and thus, reduction of flexibility would be a key prerequisite for a successful *in vivo* application. One way to stabilize aptamers is to increase thermal stability of double-stranded areas located within non-binding regions. In this respect, locked nucleic acids (LNAs) hold great promise because of their substantially increased helical thermostability and excellent mismatch discrimination when hybridized with RNA or DNA (22–26). A further advantage of LNA is its resistance to degradation by nucleases (27–29). Based on these attractive features, the LNA modification has found successful applications in antisense oligonucleotides (22,30–33), DNAzymes (34,35) and decoy

*To whom correspondence should be addressed. Tel: +49 30 83856002; Fax: +49 30 83856413; Email: erdmann@chemie.fu-berlin.de

oligonucleotides (36). Recent studies show that LNA modification within aptamers is very promising with regard to nucleolytic stability (37).

In our attempts to generate new powerful probes for *in vivo* imaging applications, we applied the LNA modification to improve the Tenascin-C aptamer TTA1 (38) with regard to *in vivo* stability, targeting function and biodistribution. TTA1 (Figure 1) is a 39mer oligonucleotide (molecular weight of 13.4 kDa) that structurally recognizes human Tenascin-C (TN-C) and binds to it with high affinity (K_d of 5×10^{-9} M) (38). TN-C is a hexameric protein found in the extracellular matrix that plays an important role in tumorigenesis, embryogenesis and wound healing (39). Based on this feature, TTA1 labelled with technetium-99m (Tc-99m) is a promising candidate for imaging of tumors expressing TN-C. The TTA1 aptamer is currently in clinical trials. Adequate stability of TTA1 against nucleolytic degradation has been achieved by replacement of all pyrimidine ribonucleotides by 2′-deoxy-2′-fluoro nucleotides and 14 of the 19 purine ribonucleotides by 2′-deoxy-2′-OMe nucleotides. Additionally, the 3′ end is blocked with a 3′-3′-thymidine cap. Further structural characteristics include a $(CH_2CH_2O)_6$ spacer and a 5′ hexyl-aminolinker. Via the latter, an N_2S peptidyl radiometal chelate (12,13) can be attached to TTA1. Limited SAR studies have been performed so far for TTA1. It has been found that the remaining 2′-ribopurines at positions 9, 11, 14 and 17 are required to maintain high affinity binding to the TN-C target (38). Modification in any of these positions with changes as small as a 2′-OH to 2′-OMe substitution leads to a significant decrease in binding. This limited SAR, coupled with aptamer truncation data, previous co-variation analysis of additional binding aptamers from the original SELEX and thermodynamic stability calculations (40) lead to the putative structure shown in Figure 1. It is a three-stem junction where the binding domain is centered on the junction. The stem I sequence is hypothesized not to be critical for binding nor are the loop structures closing stems II and III. It is supposed that the spatial localization of the TN-C target recognition involves the stem II and III regions but that stem I (Figure 1) is largely important for the structural stability of the whole aptamer and the maintenance of binding activity in the other two stem regions (38). The existence of stem I is critically important. Abolition leads to loss of binding. It cannot be ruled out that the stem plays a role in binding, just that a specific sequence does not seem to be necessary.

In the present study, further SAR experiments were carried out for TTA1. Modification of stem I (Figure 1) of TTA1 with LNA leads to a significant thermal stabilization of the stem as seen by melting experiments. In addition, the LNA modification in stem I leads to a significantly increased nucleolytic *in vivo* stability of the TTA1 while keeping the high binding affinity to TN-C. Furthermore, prolonged blood retention and increased tumor uptake have been observed in mice. In contrast, incorporation of LNA within the stems of the binding site of TTA1 (stem II and stem III) significantly increases nuclease resistance but leads to a complete loss of binding to TN-C.

MATERIALS AND METHODS

Oligonucleotide synthesis and purification

Oligonucleotides were synthesized according to the phosphoramidite method on an ABI 394 synthesizer. Oligonucleotide building blocks were obtained from Proligo (Hamburg, Germany). Purification of the oligonucleotides was carried out on a Resource 3 ml column (Amersham Biosciences) in the DMT-on mode on a Beckmann HPLC System equipped with a System Gold 168 Detector and System Gold 126 Solvent Modules. After detritylation, the oligonucleotides were purified again on a Waters XTerra™ RP18 column (5 μm, 3.9 mm × 150 mm) using a triethylammonium acetate (TEAA)/acetonitrile (ACN) buffer system (solvent A: 50 mM TEAA, solvent B: 80% ACN in solvent A) or purified by

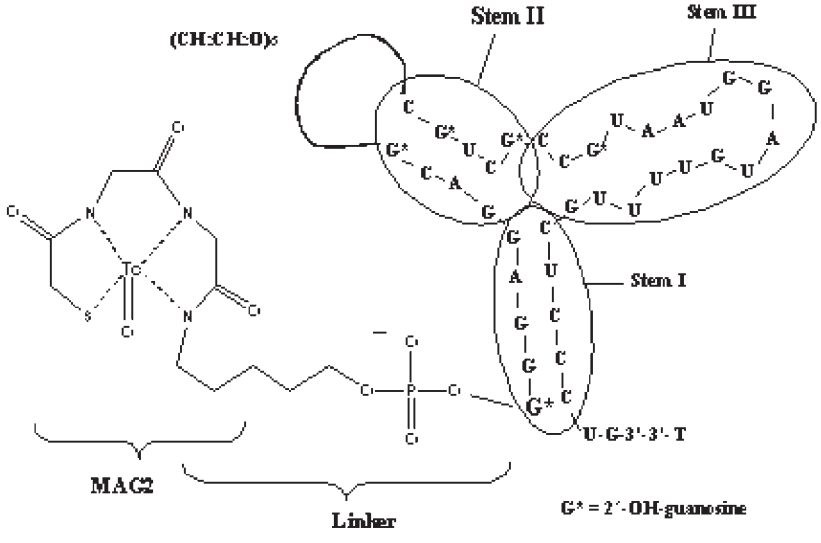

Figure 1. Structure of the TTA1 aptamer represented by 39 nt with a thymidine cap at the 3′ end and a MAG_2 chelate conjugated via an hexyl-aminolinker at the 5′ end. All pyrimidines are 2′-F nucleotides and all purines with the exception of the indicated guanosines are 2′-OMe nucleotides. The supposed stem regions I, II and III are plotted as ellipses exclusively in the $(CH_2CH_2O)_6$-loop.

denaturing (7 M urea) 12% PAGE. Large-scale synthesis of the aptamers TTA1.1 and TTA1.2 was carried out at RNA.tec (Leuven, Belgium). Furthermore, we synthesized two additional compounds (TTA1.3 and TTA1.4) differing from TTA1.2 only in that they bear additional LNA modifications in the stems II and III also (Table 1). TTA1.3 contains LNA modifications within the double-stranded regions of stems I and II (positions 1–9, 10–12 and 32–36). Like in the original TTA1, positions 14 and 17 contain ribo-guanosine. TTA1.4 contains LNA modifications in the double-stranded regions of stems 1 and 3 (positions 1–5, 19–21, 26–28 and 32–36). Here, as well, like in the original TTA1, positions 9, 11, 14 and 17 contain ribo-G. TTA1.3 and TTA1.4 contain additionally four dTs at the 5′ terminus instead of an aminolinker. This modification was done in order to get a handle for ^{32}P-labelling.

Melting curves

Melting curves of the 6mer duplexes were recorded on a Hewlett Packard Diode Array spectrophotometer 8452A in a medium-salt buffer (10 mM sodium phosphate, 100 mM NaCl, 0.1 mM EDTA, pH 7) or in a low-salt buffer (1 mM sodium phosphate, 0.1 mM EDTA) using the two complementary oligonucleotide strands at 7.5 µM. OD_{260} was measured as a function of temperature from 10 to 90°C with a 1°C increase per min. T_m values were obtained from the maxima of the first derivatives of the melting curves. HPLC analysis of the T_m samples was carried out on a Beckmann HPLC System equipped with a System Gold 168 Detector and System Gold 126 Solvent Modules using a Beckmann ODS column (5 µm, 4.6 mm × 25 cm) and detecting the oligonucleotides at 260 nm. A TEAA/ACN buffer system was used with 50 mM TEAA, pH 8 (buffer A) and 80% Acetonitrile in A (buffer B). Samples were lyophilized and desalted prior to Maldi-TOF MS analysis.

Maldi TOF analysis

Maldi-TOF MS spectra were recorded on a Voyager-DE-STR (Applied Biosystems) in the linear positive ion mode between 500 and 25 000 mass units using a laser at 337 nm, an acceleration voltage of 22 kV, a delay of 600 s and a sampling rate of 1000 MHz. External calibration was used. The samples were prepared as follows: to an aqueous solution of the oligonucleotide sample (0.2–0.3 mg/ml) were added 0.6 µl ammonium citrate solution (2.5 mg/ml) and 0.8 µl 3-Hydroxypicoline acid [10 mg/ml in ACN:H_2O (1:1)]. After mixing, the samples were applied to the target and dried for 30 s under vacuum. The following masses have been detected:

5′-($A^LC^LT^LC^LC^LC^L$) × 5′-($G^LG^LG^LA^LG^LT^L$): $(M+H)^+$ = 3978, 5′-($A^LC^LT^LC^LC^LC^L$): $(M+H)^+$ = 1936, 5′-($G^LG^LG^LA^LG^LT^L$): $(M+H)^+$ = 2041.

Table 1. TTA1 derivatives, plasma stabilities of ^{32}P-labelled TTA1 derivatives and binding affinities to TN-C

Aptamer	Modifications	Plasma stability $t_{1/2}$ (h)	Binding affinity EC_{50} (nM)
TTA1	—	42	5.8
TTA1.1	pos. 1–5, 32–36: 2′-OMe	49	13.7
TTA1.2	pos. 1–5, 32–36: LNA	53	2.0
TTA1.3	pos. 1–12, 32–36: LNA	69	No binding
TTA1.4	pos. 1–5, 19–21, 26–28, 32–36: LNA	72	No binding

Conjugation of aptamers to a MAG_2 chelator

For the preparation of the N_3S-conjugated aptamers, an *S*-^{t}Bu-protected mercapto-acetyl-glycinyl-glycine (MAG_2) compound was activated with *N*-Hydroxysuccinimide in the presence of 1-(3-Dimethylaminopropyl)-3-ethylcarbodiimide HCl (EDC). The *S*-^{t}Bu-protected MAG_2 compound was synthesized according to a literature procedure (41): 14.42 mg (30 µmol) *S*-^{t}Bu-protected MAG_2 was dissolved in 120 µl DMF. After the addition of 3.79 mg (33 µmol) *N*-Hydroxysuccinimide and 6.32 mg (33 µmol) EDC, the reaction mixture was stirred for 1 h at room temperature. An ITLC in dichloro methane and methanol (7:3) indicated complete activation. Five microliters (600 µg, 1.25 µmol) of the reaction solution were added without further purification to 1.2 mg (100 nmol) TTA1.1–5 dissolved in 20 µl sodium hydrogen phosphate buffer (0.1 M, pH 7.4). After incubation for 1 hr at 37°C, the product was purified by spin-filtration using a spin filter with a 10 kDa cut-off membrane (Microcon® MY-10, Amicon bioseparations). The residue on the filter was washed three times with water. The purity was determined by HPLC analyses. The product was deprotected using tris-(2-carboxyethyl) phosphine (TCEP) in a 10-fold molar excess (4.4 mg TCEP in 150 µl sodium acetate buffer (0.1 M, pH 6)). Purification was carried out by spin-filtration using a spin filter with a 10 kDa cut-off membrane (Microcon® MY-10, Amicon bioseparations).

Tc-99m labelling of oligonucleotides

The oligonucleotides TTA1, TTA1.1 and TTA1.2 (≈50 µg; ≈4 nmol) dissolved in 100 µl of water were mixed with 200 µl of phosphate buffer (0.1 M, pH 8.5) containing 23 mg (0.1 mmol) of L-Tartaric acid disodium salt. Tin(II) chloride (25 µg; 0.13 µmol) in 5 µl of ethanol was added to the solution. Subsequently, generator eluate (CIS bio international, Saclay, France) was added, containing 50 mCi of Tc-99m sodium pertechnetate. The kit vial was then placed into an oil bath at 95°C for 15 min. Purification was performed by spin-dialysis, employing a spin filter with a 10 kDa cut-off membrane (Microcon® MY-10, Amicon bioseparations). The residue on the filter was washed three times with water. The radiochemical purity (RCP) was determined by TLC and HPLC analyses. RCP: >95%. Yield: 40–80%. Specific radioactivity: 0.4–0.8 mCi/µg.

An Agilent 1100 HPLC system, equipped with a binary pump system, was used for purification. An RP-Eurospher 100-C18 column, 250 mm × 4 mm, was applied using Na_2HPO_4, buffer (0.01 M, pH 7.4) as solvent A and MeCN/H_2O buffer (9/1, v/v) as solvent B. A gradient from 0% B to 100% B within 20 min was applied. Detection was achieved by a γ-radioactivity detector Model:2″, S81030043, Ray-Test. TLC analysis was performed using Silica gel strips and methyl ethyl ketone (MEK) as well as water/SDS (1%) solvents. The sample was pre-spotted with water/human serum albumin (HSA) (10%).

Plasma stability

Aliquots of 100 pmol of the oligonucleotides were end-labelled with 30 µCi (γ-^{32}P)ATP using T4 polynucleotide kinase at 37°C for 45 min and purified on a 10% polyacrylamide gel with 7 M urea. Gel-purified oligonucleotides were incubated at 37°C in a final volume of 0.5 ml of freshly prepared heparinized human plasma. Samples of 20 µl were removed after 0, 0.5, 1, 3, 6, 24 and 48 h. Reactions were terminated by addition of 180 µl of loading buffer (40 µl 1× TBE, 40 µl SDS 10%, 100 µl formamide loading dye), and subsequent storage on ice. Full-length and digested oligonucleotides were separated on a 10% TBE urea polyacrylamide gel (Bio-Rad Protean IIxi cell, 1.5 mm) and autoradiographed (Figure 3). Quantitative analysis was performed on a Molecular Dynamics SI PhosphorImager system and average half-lives were calculated with WinNonLin (Pharsight, CA, USA). The goodness of regression fits was $R^2 > 0.9$.

Binding assay

A competition filter binding assay was carried out in order to determine binding constants. Samples of 2 nM human TN-C (Chemicon) were incubated with 1 nM Tc-99m-labelled TTA1 in TBSMC buffer (20 mM Tris, pH 7.4; 137 mM NaCl; 1 mM $CaCl_2$; 1 mM $MgCl_2$) and the binding competed with varying concentrations of unlabelled aptamer. Incubation was carried out at 37°C for 15 min. Subsequently, the solutions were pipetted on a Minifold Device (Schleicher and Schuell) equipped with a supported nitrocellulose membrane (BIORAD, 0.45 µm) and Whatman filter paper (Schleicher and Schuell) and washed with buffer using vacuum. Residual radioactivity due to TN-C-bound labelled aptamers on the membrane was quantified using a Phosphorimager. EC_{50} values have been calculated using GraphPadPrism 3.02 (San Diego, CA, USA) plotting one-side competition non-linear regression curves.

Biodistribution studies

The biodistributions of Tc-99m-labelled TTA1, TTA1.1 and TTA1.2 (all large-scale synthesis) were investigated in nude mice bearing subcutaneous human U251 glioblastoma. Expression of human TN-C in the U251 xenograft has previously been confirmed using an ^{125}I-anti-TN-C antibody (data not shown). Female nude mice (NMRI-Foxn1^{nu}, Taconic), of approximately 22 g body weight were inoculated with 2.2×10^6 U251 human glioblastoma cells (ATCC) in 100 µl PBS subcutanously in the right hind flank. After 3–4 weeks, mice with palpable tumors (appr. 100 mg) were injected with 74–111 kBq Tc-99m-aptamer into the tail vein. After 0.25, 1 and 5 h post-injection (p.i.), three mice were sacrificed per time-point and selected organs counted for radioactivity in a gamma-counter (Compugamma LKB Wallac). %ID/g (% injected dose per gram tissue) and %ID (% injected dose) were calculated for organs, urine and feces.

RESULTS

Melting curves

In this study, the effect of thermal stabilization of the TTA1 stem I (Figure 1) on aptamer function and stability was explored. The aim was to investigate the effect of a reduced flexibility on binding affinity and on nuclease resistance. To this end, several model hexanucleotides with 2′-F, 2′-OMe and LNA modifications representing the sequence of stem I were synthesized, and the melting temperatures of the respective hexanucleotide duplexes have been determined (Table 2). The hexanucleotide duplex consisting of 5′-GGGAGU (2′-OMe) and 5′-ACUCCC (2′-F) representing the original stem I of TTA1 displays a lower melting transition than the corresponding RNA/RNA duplex (26 vs 37°C). In comparison, the melting point of the duplex formed by two 2′-OMe modified strands is 39°C (Table 2). No data have been published so far for the hybrdization properties of LNA towards oligonucleotides containing 2′-OMe and 2′-F modifications. We have observed a significant increase of melting temperatures (Table 2) with T_Ms of 60°C and >80°C for the duplex formed by the LNA/2′-F and the LNA/2′-OMe duplexes, respectively. As expected, the highest thermal stability has been obtained with the duplex comprised of complementary all-LNA hexanucleotides (Table 2). This duplex did not denature even under denaturing reverse-phase HPLC conditions at elevated temperatures, in contrast to the corresponding RNA/RNA duplex.

Subsequently, the effect of 2′-OMe and LNA modifications on the stem I stabilization within the whole TTA1 aptamer was analyzed. We synthesized the two TTA1 derivatives TTA1.1 and TTA1.2 (Table 1) having 2′-OMe and LNA modifications, respectively, in stem I. The melting characteristics have been compared to that of TTA1 (Figure 2). In high-salt buffer (110 mM Na^+) no distinct melting transitions were observed for all three compounds. In contrast, under low-salt buffer conditions (1 mM Na^+), the melting profiles changed. Still, no clear transition could be observed for TTA1, indicating that dissociation of stem I merges with other melting transitions. However, for TTA1.1 and TTA1.2 distinct transitions could be observed at 48 and 65°C, respectively (Figure 2). These data follow the same trend as the hexamer model duplexes (Table 2). Also, here the modification of stem I with LNA leads to the highest thermal stabilization as observed for TTA1.2.

Table 2. Melting data of hexanucleotide duplexes

Duplex type	T_M[a] (°C)	T_M[b] (°C)	Duplex type
5′-r(ACUCCC)/5′-r(GGGAGU)	37	<20	RNA/RNA
5′-r(ACUCCC)/5′-(G^{L}G^{L}G^{L}A^{L}G^{L}T^L)	74	52	RNA/LNA
5′-r(GGGAGU)/5′-(A^{L}C^{L}T^{L}C^{L}C^{L}C^L)	74	53	RNA/LNA
5′-(A^{OMe}C^{F}U^{F}C^{F}C^{F}C^F)/ 5′-(G^{OMe}G^{OMe}G^{OMe}A^{OMe}G^{OMe}U^{OMe})	26	n.m.	2′-F/2′-OMe
5′-(A^{OMe}C^{OMe}U^{OMe}C^{OMe}C^{OMe}C^{OMe})/ 5′-(G^{OMe}G^{OMe}G^{OMe}A^{OMe}G^{OMe}U^{OMe})	39	n.m.	2′-OMe/ 2′-OMe
5′-(A^{OMe}C^{F}U^{F}C^{F}C^{F}C^F)/ 5′-(G^{L}G^{L}G^{L}A^{L}G^{L}T^L)	60	n.d.	2′-F/LNA
5′-(A^{L}C^{L}U^{L}C^{L}C^{L}C^L)/ 5′-(G^{OMe}G^{OMe}G^{OMe}A^{OMe}G^{OMe}U^{OMe})	>80	n.d.	2′-OMe/LNA
5′-(A^{L}C^{L}T^{L}C^{L}C^{L}C^L)/ 5′-(G^{L}G^{L}G^{L}A^{L}G^{L}T^L)	>90	>90	LNA/LNA

n.m., not measurable; n.d., not determined.
[a]10 mM sodium-phosphate, 100 mM NaCl, 0.1 mM EDTA.
[b]1 mM sodium-phosphate, 0.1 mM EDTA.

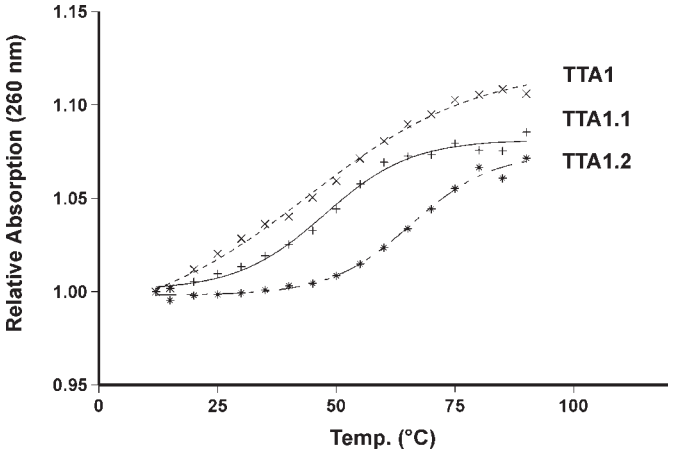

Figure 2. Melting curves of TTA1 (dotted), TTA1.1 (straight) and TTA1.2 (interrupted) recorded at 260 nm between 10 and 90°C in a low-salt buffer (1 mM sodium phosphate, 0.1 mM EDTA). Curves were plotted with GraphPadPrism 3.02 using a Boltzman-sigmoidal regression fit.

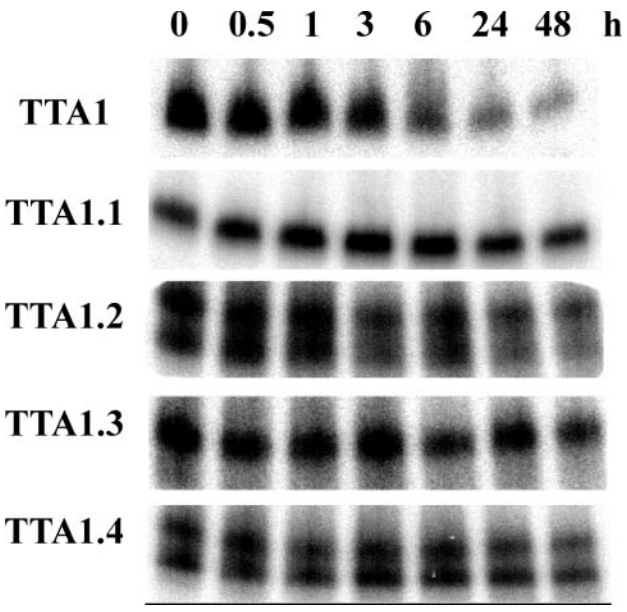

Figure 3. Analysis of the stability of TTA1 and its derivatives in human blood plasma by PAGE (see Materials and Methods). The two spots of TTA1.2 and TTA1.4 are most likely due to alternative conformations.

Stability of the aptamers in human plasma

To be effective therapeutic or diagnostic tools, aptamers must resist rapid degradation by exo- and endonucleases. Human plasma predominantly contains a 3′-exonuclease activity (42). To achieve adequate *in vivo* stability of TTA1 several features including the 3′-3′-thymidine linkage at the 3′ terminus as well as different 2′-F and 2′-OMe modifications had already been incorporated (38). In human blood plasma, phoshorylated TTA1 has an estimated half-life of 42 h as determined by PAGE analysis (Figure 3). To test the effect of further modifications on the nucleolytic stability of TTA1, plasma stabilities have been investigated for TTA1.1, TTA1.2, TTA1.3 and TTA1.4. For this purpose, the aptamers have been labelled at their 5′ end with ^{32}P. The half-lives in human plasma are summarized in Table 1. The data clearly show that the plasma stabilities of the 2′-OMe and LNA-modified TTA1 derivatives are significantly higher than that of the unmodified TTA1. Increased half-lives of ∼49 h for TTA1.1 and ∼53 h for TTA1.2 have been obtained by regression fit of data.

Binding studies for TTA1 derivatives

It has been hypothesized that aptamers with a more stable overall structure have a higher affinity to their target because the entropic penalty upon binding is lower (21). Stabilization could, however, also cause a perturbation of the binding site and thus decrease the binding affinity. To test the effect of stabilization by LNA-modification on the binding properties, we determined EC_{50} values for each TTA1 derivative by a competitive binding assay in which varying concentrations ofunlabelled aptamers competed with constant amounts of Tc-99m-labelled TTA1 in binding to TN-C. (Figure 4). The results have been listed in Table 1. The data show that LNA incorporation in stem I does not impair the binding affinity to TN-C at all. An EC_{50} of 2 nM has been calculated, which is approximately 3-fold lower as compared to the original aptamer TTA1. Even the 2′-OMe modifications within stem I had only little influence on the high binding affinity. The EC_{50} of TTA1.1 is still in the nanomolar range (∼14 nM).

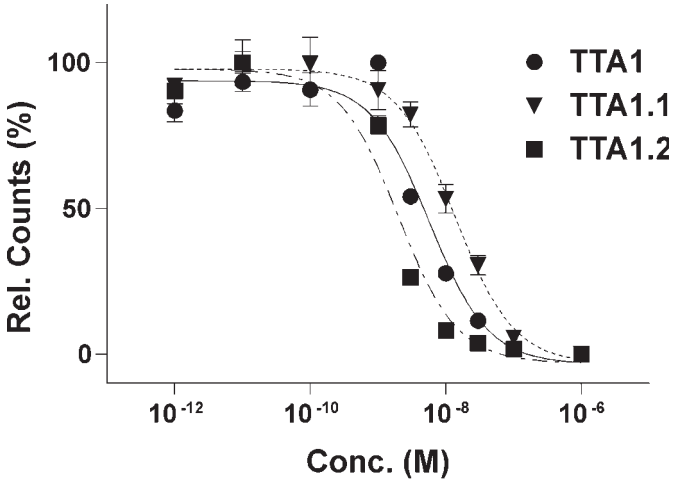

Figure 4. Binding curves of TTA1 (circles), TTA1.1 (triangles), and TTA1.2 (squares) to human Tenascin-C competing against Tc-99m-TTA1 with concentrations between 10^{-12} and 10^{-6} M. Curves were plotted with GraphPadPrism 3.02 using a one-side-binding regression fit of the means (n = 3, ±SD).

In contrast, whenever LNA was incorporated within the supposed binding regions (stems II and III) as in the case of TTA1.3 and TTA1.4, the aptamers lost their binding affinity to TN-C almost completely. This observation confirms the assumption of the 3-stem junction structure and binding regions of the TTA1 aptamer to TN-C as shown in Figure 1.

Biodistribution studies

The modified TTA1 analogs which had kept their binding affinity to TN-C (TTA1.1 and TTA1.2) were used for

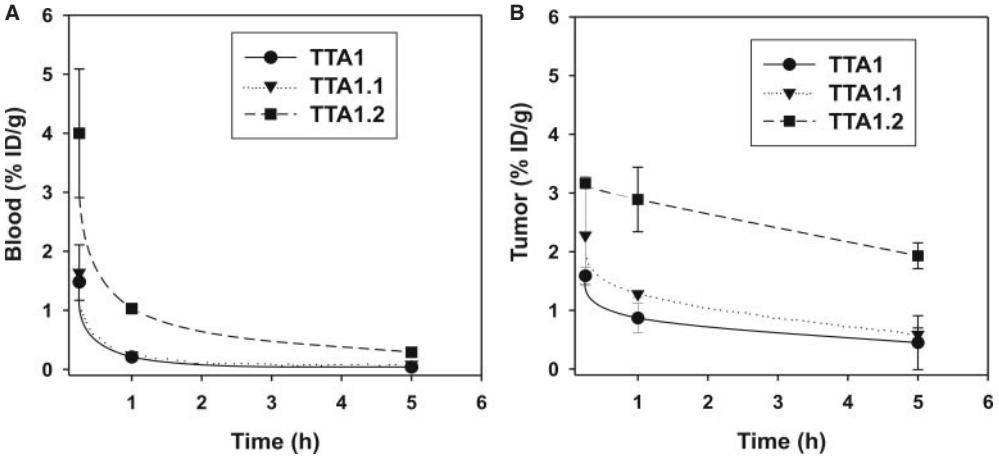

Figure 5. Blood kinetics (**A**) and tumor uptake (**B**) of TTA1 (circles), TTA1.1 (triangles), and TTA1.2 (squares) labelled with Tc-99m in U251-tumor-bearing nude mice. Values are expressed as % injected dose per gram ($n = 3$, ±SD).

in vivo biodistribution studies. TTA1.1 and TTA1.2 were conjugated to a MAG_2 chelator, labelled with Tc-99m and investigated for biodistribution in mice bearing subcutaneous U251-tumors (human glioblastoma). Since a rapid clearance of the relatively small aptamers (which have a molecular weight between peptides and single-chain antibody fragments) was expected, pharmacokinetics were investigated predominantly for early time-points (0.25, 1, 5 h). The biodistribution data of the stabilized aptamers were compared with that of TTA1. The complete data set is added as Supplementary Material (Tables 4–6). The biodistribution after 1 h will be discussed in more detail below. Whereas Tc-99m-TTA1 was characterized by a rapid blood clearance, a moderate tumor uptake (0.87% ID/g at 1 h p.i.) and a fast excretion in urine (46%) and feces (34%) especially TTA1.2 showed improved tumor uptake (2.89% ID/g at 1 h p.i.), significantly slower blood clearance (Figure 5A) and a slower excretion mainly via the urinary pathway (Table 3). The slow kinetic of the LNA-modified TTA1.2 led to an increase of unspecific uptake in all organs with the exception of the intestine. Compared to TTA1 also Tc-99m-labelled TTA1.1 depicted increased tumor uptake (1.28% ID/g, 1 h p.i.) and a high urinary excretion. However, the blood kinetics did not differ from unmodified TTA1 (Figure 5A). In contrast to TTA1, both stabilized aptamers TTA1.1 and TTA1.2 showed elevated kidney and liver uptake (Figure 6) resulting in low tumor-to-kidney and tumor-to-liver ratios. The altered excretory pathways are reflected in the low intestinal uptake of TTA1.1 and TTA1.2 compared to the unmodified aptamer TTA1 (Figure 6). Biodistribution data, in particular intestinal uptake of TTA1 and increased liver and kidney values for the modified aptamers TTA1.1 and TTA1.2, were confirmed in independent experiments with other tumor models (Tables 7–9 of the Supplementary Material).

Table 3. Biodistribution (1 h p.i. in %ID/g) and excretion (5 h p.i. in %ID) of Tc-99m-labelled aptamers

	TTA1	SD	TTA1.1	SD	TTA1.2	SD
Biodistribution (1 h p.i. in %ID/g)						
Spleen	0.44	0.14	1.59	0.63	3.98	1.07
Liver	1.12	0.04	9.73	1.46	12.63	0.37
Kidneys	0.60	0.03	21.14	4.16	20.13	3.49
Lung	0.20	0.02	0.36	0.09	1.57	0.32
Bone[a]	0.32	0.04	1.78	0.26	3.61	0.21
Heart	0.10	0.02	0.29	0.02	0.88	0.09
Brain	0.02	0.01	0.03	0.01	0.04	0.02
Fat[a]	0.06	0.03	0.33	0.10	0.25	0.09
Thyroid	0.28	0.02	0.79	0.15	2.15	0.05
Muscle[a]	0.07	0.03	0.17	0.09	0.37	0.11
Tumor	0.87	0.25	1.28	0.06	2.89	0.55
Skin	0.28	0.10	0.65	0.09	1.14	0.16
Blood	0.21	0.01	0.24	0.04	1.03	0.09
Tail	1.26	0.21	0.92	0.03	2.06	0.52
Stomach	0.22	0.10	0.84	0.03	2.54	0.49
Ovaries	0.40	0.28	0.56	0.14	1.21	0.11
Uterus	0.21	0.11	0.27	0.14	0.78	0.27
Intestine	14.79	1.05	1.13	0.22	0.65	0.09
Pancreas	—	—	0.82	0.27	0.95	0.36
Excretion (5 h p.i. in %ID)						
Urine	46.19	5.48	77.92	9.69	48.49	5.55
Feces	34.12	8.72	10.45	13.66	6.99	5.11

[a]Tissue aliquots taken only.

DISCUSSION

For a successful *in vivo* application in tumor radioimaging, an aptamer must possess acceptable *in vivo* stability against degrading enzymes as well as a tight and selective binding to its target. Furthermore, favorable *in vivo* pharmacokinetics and pharmacodynamics are required including a high signal-to-noise (e.g. tumor-to-blood) ratio. A combination of a high tumor uptake with a fast blood clearance is optimal in this respect. In the present study, we aimed at improving the TTA1 aptamer (38) with respect to *in vivo* stability, binding affinity and biodistribution. We investigated if thermal stabilization of the aptamer stem I (Figure 1), which is presumed to be not involved in target binding and recognition would lead to a conformationally and nucleolytically more stable TTA1 structure. Therefore, we have carried out structure–activity relationship studies correlating thermal stability with binding affinity and plasma stability. We analyzed melting behavior of the parental aptamer TTA1, the 2′-*O*-methyl modified aptamer TTA1.1 and the LNA-modified aptamer TTA1.2. For TTA1, we did not observe any distinct transition between 12 and 90°C

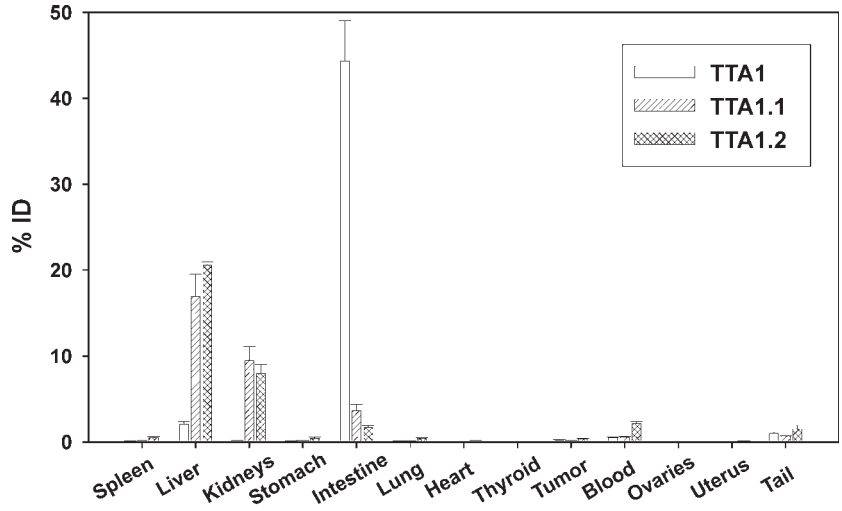

Figure 6. Biodistribution of Tc-99m-labelled TTA1 (white), TTA1.1 (stripe), and TTA1.2 (traverse) in U251-tumor-bearing nude mice. Values are expressed as % injected dose ($n = 3$, ±SD) measured 1 h post injection.

indicating that all transitions merge. In contrast, TTA1.1 and TTA1.2 show distinct transitions at 48 and 65°C, respectively (Figure 2). Thus, incorporation of 2′-OMe and LNA modifications within stem I results in a significant thermal stabilization. These results were in line with our initial model studies that showed thermal stabilities decreasing in the order LNA/LNA > 2′-OMe/2′-OMe > RNA/RNA > 2′-F/2′-OMe (Table 2).

In our attempts to correlate stem stabilization with binding affinity, it was important to see that both TTA1.1 and TTA1.2 maintain the high binding affinity to TN-C (EC_{50} values of 13.7 and 2 nM, respectively). LNA modifications within stems II and III of TTA1 lead to complete loss of binding as seen for TTA1.3 and TTA1.4. These studies support a model in which Stem I is important structurally, but is not involved in direct protein contacts and Stems II and III are more intimately associated with the protein target. Non-canonical structures are likely to occur but have not been probed at this time.

An important outcome of our study is that LNA modification in stem I within TTA1.2 renders the aptamer more resistant to nucleolytic degradation. The half-life of TTA1.2 in human blood plasma is approximately 25% higher than that of TTA1 (Table 2). Thus, the LNA modifications within stem I serve to further protect the TTA1 aptamer against enzymatic degradation. The nucleolytic stability of TTA1 was further increased when additional LNA modifications are incorporated within the binding site (stems II and III) as seen for TTA1.3 and TTA1.4 (Table 1). These half-lives are comparable with that of Spiegelmers [(43) and references therein] and exceed the half-lives of aptamers containing only 2′-F and 2′-OMe modifications (44). Thus, the application of LNA within aptamers complements other strategies to achieve adequate *in vivo* stability (e.g. applications of phosphorothioate caps, 2′-F, 2′-OMe and 2′-NH_2 modifications as well as Spiegelmers) (43–45).

Our results with regard to binding affinity and nuclease resistance can be compared to a recent study by Darfeuille *et al*. (37). There, LNA modification was applied to a short hairpin aptamer against the TAR RNA element of HIV-1. Like in our study, increased serum stability was achieved while retaining binding affinity. In contrast to TTA1, this aptamer binds via duplex formation (loop–loop interaction) to an RNA target. Therefore, partial LNA substitution within the binding site of the aptamer did not impair binding. Our study with TTA1 differs to that study in that we optimized an aptamer that binds via structure recognition to a protein target (TN-C). Therefore, it is not unexpected that LNA substitution within the binding site (stems II and III) of TTA1 leads to entire loss of target binding due to alteration of the tertiary structure.

Key prerequisites for a successful application of aptamers in molecular imaging are rapid tumor penetration and high tumor uptake. In this respect, TTA1.2 shows superior qualities compared to TTA1. In mice bearing the human glioblastoma U251, the Tc-99m-labelled TTA1.2 exhibited a three times higher tumor uptake than TTA1 (Figure 6). However, a critical parameter in tumor imaging is a high signal-to-noise (tumor-to-tissue) ratio. Due to the slower clearance of TTA1.1 and TTA1.2, the tumor-to-blood ratios were not improved as compared to TTA1 (Table 3). In contrast to the stabilized aptamers, TTA1 shows extremely rapid fecal clearance. The most likely explanation is that the RNA is being degraded and excreted through the intestine. Clearance of the modified aptamers TTA1.1 and TTA1.2 is not only slower but also dominated by urinary excretion. This altered distribution probably reflects altered stability and enhanced accumulation in kidney and liver cells due to slower degradation.

Although high accumulation in liver and kidney is reminiscent of what is commonly encountered with phosphorothioate oligonucleotide, for a successful application in tumor imaging the excretion pattern of the stabilized aptamers TTA1.1 and TTA1.2 have to be improved. An optimal imaging aptamer will probably be a compromise between a very stable molecule and a molecule in which unbound aptamer is rapidly degraded and excreted. Attempts to achieve this aim are currently underway. Nevertheless, the significantly improved *in vivo* stability and tumor uptake indicate a promising use of LNA-modified aptamers.

In conclusion, we have shown that post-SELEX modification of TTA1 with LNA within its stem I leads to improved plasma stability, high binding affinity as well as increased tumor uptake. These are essential prerequisites for a successful application of TTA1 for *in vivo* tumor imaging. It is envisaged that improvements gained for TTA1 can be be translated to other imaging aptamers.

SUPPLEMENTARY MATERIAL

Supplementary Material is available at NAR Online.

ACKNOWLEDGEMENTS

We wish to thank G. Baude (Schering AG, Berlin, Germany) for recording the MALDI-TOF MS spectra, J. Jannsen (Schering AG, Berlin, Germany) for performing the plasma stability and binding assays, B. Bieber (Free University, Berlin, Germany) for recording melting curves and M. Rimmele (RiNA GmbH, Berlin, Germany) for critically reading the manuscript. Proligo (Hamburg, Germany) is acknowledged for providing the LNA phosphoramidites. We also thank RiNA GmbH (Berlin, Germany) and RNA.tec (Leuven, Belgium) for helpful cooperations. Finally, we acknowledge Schering AG (Berlin, Germany) and the Federal Ministry of Science and Technology (BMBF) for financial support.

REFERENCES

1. Jayasena,S.D. (1999) Aptamers: an emerging class of molecules that rival antibodies in diagnostics. *Clin. Chem.*, **45**, 1628–1650.
2. Sullenger,B.A. and Gilboa,E. (2002) Emerging clinical applications of RNA. *Nature*, **418**, 252–258.
3. Rimmele,M. (2003) Nucleic acid aptamers as tools and drugs: recent developments. *Chembiochem*, **4**, 963–971.
4. Lee,J.F., Hesselberth,J.R., Meyers,L.A. and Ellington,A.D. (2004) Aptamer database. *Nucleic Acids Res.*, **32**, D95–D100.
5. Tuerk,C. and Gold,L. (1990) Systematic evolution of ligands by exponential enrichment: RNA ligands to bacteriophage T4 DNA polymerase. *Science*, **249**, 505–510.
6. Ellington,A.D. and Szostak,J. (1990) *In vitro* selection of RNA molecules that bind specific ligands. *Nature*, **346**, 818–822.
7. Daniels,D.A., Chen,H., Hicke,B.J., Swiderek,K.M. and Gold,L. (2003) A tenascin-C aptamer identified by tumor cell Selex: systematic evolution of ligands by exponential enrichment. *Proc. Natl Acad. Sci. USA*, **100**, 15416–15421.
8. White,R.R., Sullenger,B.A. and Rusconi,C.P. (2000) Developing aptamers into therapeutics. *J. Clin. Invest.*, **106**, 929–934.
9. Hicke,B.J. and Stephens,A.W. (2000) Escort aptamers: a delivery service for diagnosis and therapy. *J. Clin. Invest.*, **106**, 923–928.
10. Charlton,J., Sennello,J. and Smith,D. (1997) *In vivo* imaging of inflammation using an aptamer inhibitor of human neutrophil elastase. *Chem. Biol.*, **4**, 809–816.
11. Drolet,D.W., Nelson,J., Tucker,C.E., Zack,P.M., Nixon,K., Bolin,R., Judkins,M.B., Farmer,J.A., Wolf,J.L., Gill,S.C. and Bendele,R.A. (2000) Pharmacokinetics and safety of an anti-vascular endothelial growth factor aptamer (NX1838) following injection into the vitreous humor of rhesus monkeys. *Pharm. Res.*, **17**, 1503–1510.
12. Hilger,S., Willis,M.C., Wolters,M. and Pieken,W.A. (1999) Tc-99m-labeling of modified RNA. *Nucleosides Nucleotides*, **18**, 1479–1481.
13. Hilger,S., Willis,M.C., Wolters,M. and Pieken,W.A. (1998) Synthesis of Tc-99m labelled, modified RNA. *Tetrahedron Lett.*, **39**, 9403–9406.
14. Kühnast,B., Dollé,F., Terrazzino,S., Rousseau,B., Loc'h,C., Vaufrey,F., Hinnen,F., Doignon,I., Pillon,F., David,C., Crouzel,C. and Tavitian,B. (2000) General method to label antisense oligonucleotides with radioactive halogens for pharmacological and imaging studies. *Bioconjug. Chem.*, **11**, 627–636.
15. Tavitian,B. (2003) *In vivo* imaging with oligonucleotides for diagnosis and drug development. *Gut*, **52** (Suppl. 4), iv40–iv47.
16. Pieken,W.A., Olsen,D.B., Benseler,F., Aurup,H. and Eckstein,F. (1991) Kinetic characterization of ribonuclease-resistant 2′-modified hammerhead ribozymes. *Science*, **253**, 314–317.
17. Jellinek,D., Green,L.S., Bell,C., Lynott,C.K., Gill,N., Vargeese,C., Kirschenreuter,G., Mc Gee,D.P., Abesinghe,P., Pieken,W.A., Shapiro,R., Rifkin,D.B., Moscatelli,D. and Janjic,N. (1995) Potent 2′-amino-2′-deoxypyrimidine RNA inhibitors of basic fibroblast growth factor. *Biochemistry*, **34**, 11363–11372.
18. Klussmann,S., Nolte,A., Bald,R., Erdmann,V.A. and Fuerste,J.P. (1996) Mirror-image RNA that binds D-adenosine. *Nat. Biotechnol.*, **14**, 1112–1115.
19. Nolte,A., Klussmann,S., Bald,R., Erdmann,V.A. and Furste,J.P. (1996) Mirror-design of L-oligonucleotide ligands binding to L-arginine. *Nat Biotechnol.*, **14**, 1116–1119.
20. Kim,S.J., Kim,M.Y., Lee,J.H., You,J.C. and Jeong,S. (2002) Selection and stabilization of the RNA aptamers against the human immunodeficiency virus type-1 nucleocapsid protein. *Biochem. Biophys. Res. Commun.*, **291**, 925–931.
21. Eaton,B.E., Gold,L. and Zichi,D.A. (1995) Let's get specific: the relationship between specificity and affinity. *Chem. Biol.*, **2**, 633–638.
22. Petersen,M. and Wengel,J. (2003) LNA: a versatile tool for therapeutics and genomics. *Trends Biotechnol.*, **21**, 74–81.
23. Koshkin,A.A., Singh,S.K., Nielsen,P., Rajwanshi,V.K., Kumar,R., Meldgaard,M., Olsen,C.E. and Wengel,J. (1998) LNA (Locked Nucleic Acids) synthesis of the Adenine, Cytosine, Guanine, 5-Methylcytosine, Thymine and Uracil bicyclonucleoside monomers, oligomerisation, and unprecedented nucleic acid recognition. *Tetrahedron*, **54**, 3607–3630.
24. Koshkin,A.A., Rajwanshi,V.K. and Wengel,J. (1998) Novel convenient synthesis of LNA [2.2.1] bicyclo nucleosides. *Tetrahedron Lett.*, **39**, 4381–4384.
25. Braasch,D.A. and Corey,D.R. (2000) Locked nucleic acid (LNA): fine-tuning the recognition of DNA and RNA. *Chem. Biol.*, **55**, 1–7.
26. Koshkin,A.A., Nielsen,P., Meldgaard,M., Rajwanshi,V.K., Singh,S.K. and Wengel,J. (1998) LNA (Locked Nucleic Acid): an RNA mimic forming exceedingly stable LNA:LNA duplexes. *J. Am. Chem. Soc.*, **120**, 13252–13253.
27. Wahlestedt,C., Salmi,P., Good,L., Kela,J., Johnsson,T., Hokfelt,T., Broberger,C., Porreca,F., Lai,J., Ren,K., Ossipov,M., Koshkin,A., Jakobsen,N., Skouv,J., Oerum,H., Jacobsen,M.H. and Wengel,J. (2000) Potent and nontoxic antisense oligonucleotides containing locked nucleic acids. *Proc. Natl Acad. Sci. USA*, **97**, 5633–5638.
28. Kumar,R., Singh,S.K., Koshkin,A.A., Rajwanshi,V.K., Meldgaard,M. and Wengel,J. (1998) The first analogues of LNA (locked nucleic acids): phosphorothioate-LNA and 2′-thio-LNA. *Bioorg. Med. Chem. Lett.*, **8**, 2219–2222.
29. Kurreck,J., Wysko,E., Gillen,C. and Erdmann,V.A. (2002) Design of antisense oligonucleotides stabilized by locked nucleic acids. *Nucleic Acids Res.*, **30**, 1911–1918.
30. Frieden,M., Christensen,S.M., Mikkelsen,N.D., Rosenbohm,C., Thrue,C.A., Westergaard,M., Hansen,H.F., Orum,H. and Koch,T. (2003) Expanding the design horizon of antisense oligonucleotides with alpha-L-LNA. *Nucleic Acids Res.*, **31**, 6365–6372.
31. Jepsen,J.S. and Wengel,J. (2004) LNA-antisense rivals siRNA for gene silencing. *Curr. Opin. Drug Discov. Devel.*, **7**, 188–194.
32. Hansen,J.B., Westergaard,M., Thrue,C.A., Giwercman,B. and Oerum,H. (2003) Antisense knockdown of PKC-alpha using LNA-oligos. *Nucleosides Nucleotides Nucleic Acids*, **22**, 1607–1609.
33. Grunweller,A., Wyszko,E., Bieber,B., Jahnel,R., Erdmann,V.A. and Kurreck,J. (2003) Comparison of different antisense strategies in mammalian cells using locked nucleic acids, 2′-*O*-methyl RNA, phosphorothioates and small interfering RNA. *Nucleic Acids Res.*, **31**, 3185–3193.
34. Vester,B., Lundberg,L.B., Sorensen,M.D., Babu,R., Douthwaite,S. and Wengel,J. (2002) LNAzymes: incorporation of LNA-type monomers into DNAzymes markedly increases RNA cleavage. *J. Am. Chem. Soc.*, **124**, 13682–13683.
35. Schubert,S., Gul,D.C., Grunert,H.P., Zeichhardt,H., Erdmann,V.A. and Kurreck,J. (2003) RNA leaving '10–23' DNAzymes with enhanced stability and activity. *Nucleic Acids Res.*, **31**, 5982–5992.

36. Crinelli,R., Bianchi,M., Gentillini,L. and Magnani,M. (2002) Design and characterization of decoy oligonucleotides containing locked nucleic acids. *Nucleic Acids Res.*, **30**, 2435–2443.
37. Darfeuille,F., Hansen,J.B., Orum,H., Di Primo,C. and Toulme,J.J. (2004) LNA/DNA chimeric oligomers mimic RNA aptamers targeted to the TAR RNA element of HIV-1. *Nucleic Acids Res.*, **32**, 3101–3107.
38. Hicke,B.J., Marion,C., Chang,Y.-F., Gould,T., Lynott,C.K., Parma,D., Schmidt,P.G. and Warren,S. (2001) Tenascin-C aptamers are generated using tumor cells and purified protein. *J. Biol. Chem.*, **276**, 48644–48654.
39. Erickson,H.P. and Bourdon,M.A. (1989) Tenascin: an extracellular matrix protein prominent in specialized embryonic tissues and tumors. *Annu. Rev. Cell Biol.*, **5**, 71–92.
40. Mathews,D.H., Sabina,J., Zuker,M. and Turner,D.H. (1999) Expanded sequence dependence of thermodynamic parameters improves prediction of RNA secondary structure. *J. Mol. Biol.*, **288**, 911–940.
41. Hilger,C.S., Willis,M.C., Wolters,M. and Pieken,W.A. (1999) Tc-99m labeling of modified RNA. In Nicolini,M. and Mazzi,U. (eds), *Technetium, Rhenium and Other Metals in Chemistry and Nuclear Medicine*. SG Editoriali, Padova, Vol. 5. pp. 557–560.
42. Eder,P., DeVine,R., Dagle,J. and Walder,J. (1991) Substrate specificity and kinetics of degradation of antisense oligonucleotides by a 3′ exonuclease in plasma. *Antisense Res. Dev.*, **1**, 141–151.
43. Eulberg,D. and Klussmann,S. (2003) Spiegelmers: biostable aptamers. *Chembiochem*, **4**, 979–983 and references cited.
44. Green,L.S., Jellinek,D., Bell,C., Beebe,L.A., Feistner,B.D., Gill,S.C., Jucker,F.M. and Janjic,N. (1995) Nuclease-resistant nucleic acid ligands to vascular permeability factor/vascular endothelial growth factor. *Chem. Biol.*, **2**, 683–695.
45. Bishop,J.S., Guy-Caffey,J.K., Ojwang,J.O., Smith,S.R., Hogan,M.E., Cossum,P.A., Rando,R.F. and Chaudhary,N. (1996) Intramolecular G-quartet motifs confer nuclease resistance to a potent anti-HIV oligonucleotide. *J. Biol. Chem.*, **271**, 5698–5703.